AE-30

Metallographic Study of the Isothermal Transformation of Beta Phase in Zircaloy-2

G. Östberg

AKTIEBOLAGET ATOMENERGI

STOCKHOLM · SWEDEN · 1960

Metallographic Study of the Isothermal Transformation of Beta Phase in Zircaloy-2

G. Östberg *)

Summary:

Observations of the structure of commercial zircaloy-2 have been made in the microscope showing that the high temperature beta phase is transformed isothermally at lower temperatures into alpha plus secondary precipitate. The alpha occurs mainly as Widmanstätten plates developed by a shear mechanism. The secondary precipitate is formed from the beta - alpha structure at the phase boundary between these phases. This precipitation of particles of secondary phase occurs on account of a eutectoid reaction, alpha also being formed. A time-temperature-transformation diagram has been constructed from the observations.

*) Research metallurgist, Department of Materials Research and Development, Aktiebolaget Atomenergi, Sweden.

Completion of manuscript in April 1960

Printed and distributed in May 1960

LIST OF CONTENTS

Metallographic Study of Isothermal Transformation of Beta Phase in Zircaloy-2.

Introduction.

Zircaloy-2 is a zirconium base alloy containing 1.5 % tin, 0.12 % iron, 0.05 % nickel and 0.10 % chromium. Because of its low thermal neutron absorption and good corrosion resistance in high temperature water it can be used as a cladding material for fuel elements in water cooled nuclear reactors. The structure after slow cooling to room temperature consists of a matrix of hexagonal alpha zirconium, with part of the alloying elements in solution, plus a secondary precipitate. At more rapid cooling the alloy is α zirconium with the various alloying elements in supersaturated solution. The alpha phase and secondary precipitate are formed by transformation of the high temperature beta solid solution which has body centered cubic structure. This paper reports a study of the isothermal transformation of beta at lower temperatures.

1. Previous Work.

There seems to be no investigation of the isothermal transformation of beta in zircaloy-2 reported in the literature. Other related information is however available concerning the temperature ranges of the different stages of transformation, the microstructure and mechanism of formation of alpha, and the nature of the secondary precipitate.

As to the temperature limits, the published figures are tabulated below. They are based on dilatometric measurements and microscopic observations. A typical dilatometer curve for zircaloy-2 during cooling is shown in Fig. 1. The interpretation of the critical points given in the caption is supported by evidence in the literature and by the present investigation *). Some of the dilatometric measurements reported have been made with different rates of cooling, allowing an extrapolation to very slow cooling, recorded as 0 ^{o}C/h in Table I.

*) This general interpretation of the dilatation curve is that given by Intrater (3). On the other hand Thomas & Forscher (6) as well as Mc Geary (9) regard the point C, not A, as the terminal of alpha formation during cooling.

Table I. Transformation temperatures in zircaloy-2 during slow cooling or long time of annealing, according to the literature.

Transformation	Temperature °C	Method of investigation: d = dilatometric m = microscopic	Note: contents in weight per cent; cooling rates	Ref.
Alpha:				
Start of formation	1000 - 1040	m	0.17 % O	1
	av. 1020			
	955 - 1005	m	0.10 % O	1
	av. 985			
	970	m		2
	930 - 985	m	0.05 % O	1
	av 960			
	960	d	0 °C/h	3
	942	d	100 °C/h *)	4
	(870	m (hot stage)		5)
End of formation	840	m	0.17 % O	1
	835	m	0.10 % O	1
	825	m	0.05 % O	1
	< 805	m		3
	790	d	0 °C/h	3
	783	d	100 °C/h *)	4
	780	d	100 °C/h	6
Secondary precipitate:				
Start of formation	870	d	100 °C/h	6
	854	d	100 °C/h *)	4
	850	d	0 °C/h	3

* 1.53 % Sn, 0.16 % Fe, 0.09 % Cr, 0.05 % Ni, 0.088 % O, 0.004 % N, 0.040 % C.

Transformation	Temperature °C	Method of investigation:	Note: contents in weight per cent; cooling rates	Ref.
Presence of sec. prec. found, +, and not found, -, in the microscope	- 981	m	low 0 content**)	7
	- 870	m		7
	+ 850***)	m***)		3, 5
	+ 843	m	****)	8
	- 840	m		2
	+ 780	m		3
	+ 760	m	low 0 content**)	7
	+ 750***)	m***)		5

**) Alloy based on pure crystal bar zirconium with a lower oxygen content than commercial sponge zirconium. The observations were made on specimens heated to the temperature in question and then quenched.

***) In hot stage microscope (5) no secondary precipitate was visible at 650, 750 and 850 °C, although the phase was observed in sections of the same specimens, when quenched to room temperature.

****) 1.2 - 1.7 % Sn, 0.07 - 0.20 % Fe, 0.05 - 0.15 % Cr, 0.03 - 0.08 % Ni, 0.17 % O, 0.008 (max. 0.010) % N.

Table I shows that the temperatures for the beginning and the end of formation of alpha are 940 - 990 °C and 780 - 835 °C respectively. The large variation among the published figures is believed to depend mainly on differences in composition of the alloys studied. Only in some cases, notified in the table, the deviations from the nominal composition of zircaloy-2 have been given in the references. Oxygen has a very great influence on the transformation temperatures particularly on the $\beta \rightarrow \alpha + \beta$ transformation as shown in Fig. 2. The oxygen contents in commercial zircaloy-2 range from 0.07 to 0.2 %. The influence of nitrogen is similar, but the nitrogen content is usually limited to 0.01 % to maintain corrosion resistance.

The secondary precipitate begins to form between 850 and 870 °C during cooling according to Table I. This limit lies within the $\alpha + \beta$ range, i.e. the precipitation of the secondary phase occurs parallell with the formation of alpha. The simultaneous formation of the two phases is discussed further below.

Since high temperature beta in zircaloy-2 cannot be retained to room temperature by fast cooling, the microstructure of this phase has to be studied by hot stage microscopy. One such investigation has been published (5). Beta at 1000 °C was found to have a smooth surface with no details.

The alpha phase which forms by cooling to room temperature normally appears as Widmanstätten plates. Equiaxed grains are found in zircaloy-2 that has been annealed for a relatively long time in the α- or in the $\alpha + \beta$-range (2). (In unalloyed zirconium equiaxed alpha grains are found even after fast cooling. Increasing amounts of other elements do, however, render the structure more acicular. Annealing has the same effect on this acicular structure as in zircaloy-2 (10)).

As to the mechanism of formation of the alpha plates in zirconium some indications of a martensitic shear process have been reported. When unalloyed zirconium or zirconium with some impurity content was subjected to a $\beta \rightarrow \alpha$ transformation a surface relief of alpha plates could be observed on a prepolished specimen surface (10) (11) (12) (13). Zircaloy-2

as studied in hot stage microscope (5) exhibited the same phenomenon, indicating a shear process. In Zr-Fe-alloys a surface relief occurred together with a precipitation of a secondary intermetallic phase (11)

The nature of the secondary phase in zircaloy-2 is not accurately known, although some attempts to isolate and analyze it have been made. In the Zr-Sn-Fe system the probable corresponding intermetallic phase is theta with the approximate composition 67.5 % Zr, 25 % Sn and 7.5 % Fe (14). Iron, nickel and chromium in zircaloy-2 are believed to be interchangeable in this compound. Beside the theta phase there may also exist other precipitated phases such as $ZrFe_2$, $ZrCr_2$ or Zr_2Ni. Carbide is to be expected when the carbon content, as it often does, exceeds the solubility limit which is near 0.02 % C.

Finally the literature contains some information on the type of transformation reaction, producing the two phases alpha and secondary precipitate. As mentioned above the latter begins to form, when there is still some beta left. If then the two transformation products alpha and precipitate are found cooperatively, the reaction may be either eutectoid (beta decreasing and alpha increasing in amount during the precipitation of the secondary phase) as in the binary systems Zr-Fe, Zr-Ni and Zr-Cr, or peritectoid as in Zr-Sn (alpha decreasing in amount).

The only existing experimental basis for a decision on this point is a phase diagram for the Zr-Sn-Fe system (14). The application of this diagram to zircaloy-2 requires three assumptions. First, iron is substituted for nickel and chromium. Secondly, since the composition of such "modified" zircaloy-2 falls in the α field of the Zr-Sn-Fe diagram at the temperatures of interest, 800 and 900 ^{o}C, and not in the $\alpha + \beta + \Theta$ field the arguments must concern an alloy of higher Sn and Fe contents. It is therefore assumed that conclusions about such a three phase alloy are valid also for zircaloy-2. Thirdly, for a decision on the character of three phase reactions during cooling in a ternary system, it is necessary - as pointed out by Kuo (15), and Hillert (16) - to know how all participating phases change their composition. The behaviour in this respect is known for alpha and beta but not for theta. The change in composition of theta can be assumed to be negligible, however.

In Fig. 3 the $\alpha + \beta + \Theta$ field in isothermal sections of the ternary diagram Zr-Sn-Fe at 800 and 900 °C are shown (14). Arrows indicate the change in composition of alpha and beta on cooling. Both phases increase their iron content (as in the binary system Zr-Fe) and decrease their tin content (as in the binary system Zr-Sn). An analysis of the changes in the amounts of respective phases according to Hillert (16) shows a eutectoid reaction at both temperatures.

2. Experimental Details.

The zircaloy-2 studied was made by Imperial Chemical Industries Ltd, England, from zirconium sponge, melted in vacuum and rolled to sheet. The composition is listed below. The analyses are those of the manufacturer except for carbon, in which case determinations were made in this investigation.

Table II. Composition of zircaloy-2 in weight per cent.

Sn	1.42	(nominal content in zircaloy-2 : 1.5)
Fe	0.11	(d:o 0.12)
Cr	0.09	(d:o 0.10)
Ni	0.04	(d:o 0.05)
O	0.165 - 0.170	
N	0.007	
C	0.018 - 0.066	
H	0.0070 - 0.0080	

Al, Cu, Hf and Mo less than 0.007

Cd, Co, Pb, Mg, Mn, Si, Tl, W and V less than 0.0025

B, Na and U were not determined.

The composition is close to that of normal commercial zircaloy-2, except for the oxygen content which is high.

The thickness of the sheet used in most of the experiments was 0.8 mm It was annealed and pickled. In order to make possible the necessary fast attainment of temperature at short transformation times sheet with reduced thickness, 0.3 mm, was also used.

Special alloys were prepared by arc furnace melting of zirconium or zircaloy-2 together with certain additions: one binary alloy of Zr and 0.75 % Sn and three alloys consisting of zircaloy-2 plus 0.3 % Sn, plus 0.1 % Fe and plus 0.3 % Sn and 0.1 % Fe respectively.

The normal heat treatment cycle involved as the first step a 12 min. annealing at 1050 °C to completely transfer the alloy into beta state and as the second an isothermal annealing at various predetermined constant temperatures between 100 and 990 °C. The heat treatment at 1050 °C was made in streaming argon with bare specimens. The temperature was controlled within ± 3 °C at 1050 °C. The argon was purified by passing over calcium chips at 600 and 300 °C, removing oxygen and nitrogen, and hydrogen respectively. The only detectable contamination of the specimens during the 15 min. (total time in the furnace) at 1050 °C was in a thin surface layer. The specimens were attached to a wire of zircaloy-2 and were transferred directly through the air to the isothermal annealing bath of molten tin or, at 200 °C a eutectic mixture of tin and lead. The tin bath was deoxidized by calcium and covered with charcoal. Analyses of tin and carbon in annealed material indicated that no changes took place during annealing. The isothermal temperature was controlled within ± 2 °C and 500 °C and ± 3 °C at 1000 °C. For annealings at 100 °C boiling water was used as medium in the bath. The annealing time was measured as the total time in the bath after which the treatment was finished by quenching the specimen in water at room temperature.

Observations in the microscope were made on sections polished electrolytically in a NH_4F electrolyte (17) and etched in mixtures of HF, HNO_3 and glycerine. *) The proportions of HF and HNO_3 were chosen with consideration to the details of the structures observed. It was found that high HF:HNO_3 ratios caused the secondary precipitate to stand up in relief. Larger proportions of HF gave etching products which could be neither dissolved during etching nor removed by ultrasonic vibration (in alcohol). A final rinsing with a 10 per cent solution of aluminium nitrate in water eliminated them, probably by dissolution.

---

*) Mixtures of nitric acid and glycerine are explosive if not handled with care. Recommendations for use are found in Schrader's Ätzheft (18).

Quantitative measurements of the amount of alpha were performed by lineal analysis using an apparatus of Molinder's design (19). To establish the average percentage of alpha phase a length of 2 to 3 mm was traversed in each specimen.

A limited number of specimens were studied in an electron microscope. The instrument used was the RCA type EMU 2 D at the Swedish Institute for Metal Research. Plastic replica were prepared of specimen surfaces which had been polished and etched in the same manner as for observation in a light microscope. The preparation procedure has been described in detail elsewhere (20).

Heat treatments were also made with polished specimens in order to observe the possible occurence of relief effects during transformation. Fiducial lines were made on the polished surface by scratching on a lap with three micron diamond powder. The heat treatment was carried out in a closed silica tube connected with a vacuum pump, capable of evacuating down to 7×10^{-7} mm Hg. Before the heat treatment the tube was refilled with pure argon to a pressure of approximately 10^{-2} mm Hg. The vertical silica tube was surrounded by an upper furnace giving a temperature of 1020 ^{o}C and a lower furnace for isothermal treatment at various temperatures below 950 ^{o}C. The specimen was attached to a magnet for its manipulation inside the tube. The cooling after the isothermal annealing was made by lowering the specimen into an externally water cooled chamber.

3. Results.

A survey of the phase changes observed is given in the time-temperature-transformation-diagrams, Figs. 4 and 5. Passing from high to low temperatures at longer times, where the structure is close to equilibrium, the phases replace one another in the following order: β, $\alpha + \beta$ + secondary precipitate, and finally α + secondary precipitate. The secondary precipitate is called X in this paper.

The temperature limits found compare with literature data in the following way:

	This investigation °C	Literature °C
$\beta \rightarrow \alpha + \beta$	985	940 to 985 (0.10 % O) to 1020 (0.17 % O)
$\alpha + \beta \rightarrow \alpha + \beta + X$	880	850 to 870
$\alpha + \beta + X \rightarrow \alpha + X$	810	780 to 835 (0.10 % O) to 840 (0.17 % O)

The zircaloy-2 used in this study contained 0.17 % O. With regard to the oxygen content the $\beta \rightarrow \alpha + \beta$ limit found is low, while the temperature for the beginning of precipitation of X is on the higher side. The temperature where the last β disappears coincides with the earlier findings.

Before going into the details of the structural transformations two general remarks will be made on the isothermal annealing technique. When a sample is quenched at the end of the holding time at a certain temperature the cooling rate is zero at the start and then increases. If the starting temperature lies just above a transformation range where the transformation is fast, the latter will be passed with a relatively low rate of cooling permitting phase changes in this range of fast transformation. The quenching technique is thus bound to give a false impression of the structure at quenching temperatures just above the upper limit of a range of fast transformation.

Determination of the Beta Treatment Temperature.

The minimum temperature for obtaining a single phase beta structure was determined by heating specimens to different temperatures between 950 and 1050 °C and quenching them after 12 min. time at the temperature. At 950, 970 and 980 °C there remained some unresolved alpha phase in the form of equiaxed grains aligned in the rolling direction of the sheet. Fig. 6 shows the structure at 970 °C. Alpha is the light phase. The dark matrix was beta at 970 °C but has transformed during the quench into very fine Widmanstätten alpha plates. With rising temperatures the equilibrium amount of alpha decreased. At 980 °C only small remains of alpha were left and at 1000 and 1050 °C the structure consisted only of beta. In Figs. 7 and 8 the structure of quenched beta from 1050 is shown. At high mag-

nification the alpha appears as fine plates and as a rim in a former beta grain boundary. The latter will be dealt with in detail later.

As a conclusion of these runs 12 min. at 1050 °C was chosen for transforming the structure into single phase beta prior to the isothermal annealing.

The Single Phase Beta Structure.

The grains of beta at high temperature are recognized in quenched samples by the acicular structure of the alpha which forms during the quench. A beta grain is thus distinguished by certain directions (habit planes) of the alpha plates belonging to it. Since the direction of an alpha plate is related to its lattice orientation, a certain pattern of the anisotropic alpha phase in a beta grain can be observed in polarized light. Fig. 7 illustrates this effect in a sample quenched from 1050 °C. The structure is the same in quenched, single phase beta which is retained at lower temperatures in the short time before its isothermal transformation has started, see Fig. 9.

The size of the beta grains in specimens heated at 1050 °C for 12 min. is relatively large: 8 grains per mm^2 or No. 0 according to the ASTM scale. Prolonged holding (1 h) at 1050 °C, leads to a slight increase in grain size. At 1000 and 990 °C (1 min. at temperature) the grain size is somewhat smaller than at 1050 °C, although not very much. At 1000 °C the grain size is not influenced by holding time between 12 min. and 1 h. The grain size of beta retained at lower temperatures for a short time before the start of isothermal transformation is the same as the one established at 1050 °C.

In this connection a remark should be made also on the size of the areas of equioriented alpha plates. These areas, see Fig. 7, are made up of separately formed parallell plates. Although the approximately equiaxed colonies of alpha plates of a certain direction are interconnected at some points, the difference in orientation of adjoining areas give the impression of an "alpha grain size"within the beta grain size. In specimens quenched from 1050 °C this "alpha grain size" is A. S. T. M. No. 7 to 6, corresponding to 512 to 1024 grains per mm^2 or 64 to 128

"alpha grains" per each beta grain. The "alpha grain size" in quenched beta is independent of the temperature and time of the annealing in the beta range.

This "alpha grain size" seems to be more significant than the size of the individual plates from the view point of deformation by twinning. Fig. 10 shows twins crossing a colony of equioriented alpha plates regardless of the boundaries between the individual plates, as marked by precipitated secondary phase (black or white particles).

Rim of Alpha in Beta Grain Boundaries.

Before dealing with the main form of alpha, the Widmanstätten plates, an account will be given of the already mentioned alpha rim in beta grain boundaries. Illustrations of the rim are found in Figs. 8, 9 and 12.

The rim usually etches deeper than the surrounding matrix although sometimes the difference is only slight. The lattice orientation of the rim alpha, as observed in polarized light, may be constant over considerable distances along the grain boundary, up to 100 microns. The orientation does not depend on the curvature of the boundary, nor does it always change if another boundary intersects. When the lattice orientation changes, the transition is discontinous. Widmanstätten plates growing from the rim into the beta grain, see Figs. 11 and 12, have the same lattice orientation as the rim alpha. No crystal grain boundary can be seen between the rim alpha and the Widmanstätten plate alpha. This is true even in cases where the plates extend from both sides of the rim between two adjoining beta grains. This remarkable observation was not depending upon the etching technique, since the continuity could be observed also in unetched specimens by means of polarized light.

The thickness of the rim varies along the boundary, and sometimes the rim decreases in thickness until it vanishes completely. The mean width of the rim is about 1 micron in samples quenched from single phase beta at 1050 ^{o}C, independent of holding time between 12 min. and 1 h. At 990 and 1000 ^{o}C the rim is about twice as thick as at 1050 ^{o}C.

As to the formation of the rim the observations indicate that it takes place early during cooling. The rim is certainly not present at the beta treatment temperature as an equilibrium remnant of previously existing alpha, since such alpha should not be expected to have the form of a rim but rather equiaxed grains as shown in Fig. 6. During the quench the rim forms quite early. This conclusion is partly based on the observation of the deeper etching effect on the rim alpha as compared with plates formed isothermally at lower temperatures, including the very fine ones in quenched samples. It is known, from specimens which unintentionally were transformed to alpha plates at various low temperatures, that the depth of the etch diminished with decreasing temperatures. Furthermore the rim preceeds the isothermal Widmanstätten plates at high temperature.

It is therefore concluded that the rim is a transformation product of beta which forms early during quenching or isothermally before the Widmanstätten plates. The thickness of the rim is determined by the length of time which is spent in the high temperature range where the rim is developed. Under isothermal transformation the rim soon enters into competition with faster growing Widmanstätten plates. In all observed cases only a short time has been available for the rim to grow before the plates have started to form. In the transformation diagram the time for the beginning of transformation into alpha applies to the Widmanstätten variety.

Again the orientation identity between the rim alpha and the Widmanstätten plates on one hand and the relationship between the Widmanstätten plates and the beta phase is emphasized.

Isothermal Widmanstätten Alpha Plates.

The above mentioned lattice orientation and habit relationships described for Widmanstätten alpha in samples quenched from beta are common also to the isothermally formed alpha. Figs. 11 and 12 show that isothermal alpha plates have the same direction of their main extension as the quench-formed fine plates. High temperature isothermal alpha plates are shown in Figs. 13 - 15. The plates have the shape of

lancets rather than lenses. Their ends are sometimes rounded, sometimes cut off sharply and sometimes split up in two points or more. At high temperatures the first Widmanstätten plates grow from the grain boundary rim. The start of such plates is a "sawtooth" which later takes the shape of a plate, see Figs. 11 and 12 from 980 °C. In Fig. 12 the zig-zag form of the grain boundary between two beta grains is probably the result of a movement of the boundary between the points where alpha has first been precipitated. Although the thinner plates developed during the quench are one order of magnitude finer than the isothermal plates, they are not as fine as those formed after a fast quench from beta. Probably the specimen has not been cooled fast enough from 980 °C to avoid formation of alpha plates when passing the region of fast transformation just below the isothermal level.

The influence of decreasing formation temperature on the Widmanstätten structure is to make the plates finer, i.e. thinner and shorter, if compared at the same length of time after the transformation has started.

For similar degrees of transformation the spacing between plates of the same lattice orientation and direction decreases with decreasing holding temperature. Low temperature isothermal alpha structures are shown in Figs. 15-17. (It should be borne in mind however, when examining structures in this respect that the variation in size and spacing of the plates in one single specimen is great.)

The examples described above are taken from equilibrium alpha-beta-structures, marked by a full triangle in the transformation diagram, Fig. 4. The same features apply to the Widmanstätten plates of supersaturated alpha, marked in the diagram by an open circle, and to the structures comprising both alpha plates and secondary precipitate, marked by a full circle or a square. The change in size of the alpha plates with temperature is continous and smooth even when passing from one phase combination to another.

The term supersaturated is used for the low temperature alpha phase in order to indicate that it remains a single phase solid solution for a long time after complete transformation of beta before the rejection of a precipitate, which is assumed to be X. The determination of the beginning of the formation of supersaturated alpha is a delicate question, since at lower temperatures the size of the isothermal alpha plates approaches that of the alpha plates formed during quenching of beta. However, a careful observation reveals when the transition from beta to isothermal supersaturated alpha occurs as marked by the introduction of larger alpha plates in the structure. The size of isothermal supersaturated alpha plates decreases with decreasing temperature; at longer holding times the isothermally formed plates seem to increase in size. These size criteria have, together with hardness measurements, dealt with in more detail below, been used for the determination of the range of supersaturated alpha shown in Figs. 4 and 5. There is admittedly a great uncertainty in the microscopical determination since the variations in size of the alpha plates are difficult to assess. This is particularly true of the lowest temperatures studied, 200 and 100 ^{o}C. At both these temperatures the alpha plates were found to have about the same size as in quenched beta independently of the holding time. Then the structure at 200 and 100 ^{o}C could either have been beta at these temperatures, forming fine alpha on quenching at some temperature between 100 and 20 ^{o}C, or have been developed during cooling from 1050 ^{o}C, slightly before the 200 and 100 ^{o}C levels were reached.

The position of the curve for the beginning of the isothermal formation of alpha could be more firmly established with the help of hardness determinations. The hardness was measured with a Bergsman microhardness tester (21), using a diamond pyramid indenter with a 50 g load. At 400 and 300 ^{o}C the hardness values in specimens of the shortest holding time i.e. quenched beta, were grouped between 250 to 280 Vickers units, while the isothermal alpha had hardness values at a lower level between 210 and 240. At 200 ^{o}C the 1.1 sec. specimen had a hardness of 262, indicating quenched beta, and the 10 sec. specimen 236, indicating isothermally formed alpha.

Some observations of the mode of crystallization of isothermal Widmanstätten plates have been made on specimens which had been polished before the heat treatment. Fig. 18 shows the relief produced on a previously plane surface by the formation of alpha plates. The surface is slightly tarnished by interaction of the atmosphere during the heat treatment; the small particles on the surface are probably oxide. The relief structure exactly resembles that of alpha plates in surface is polished and etched in the usual manner.

The scratches, which also existed before the transformation, are broken at the points where they cross the boundary of a plate. The observed relief together with the breaks in the fiducial lines are taken as a proof that the alpha plates have formed according to a shear mechanism, a "martensitic" process. The rim of alpha in the beta grain boundaries did not exhibit this feature.

Residual Beta at High Degrees of Transformation.

The fine Widmanstätten structure of transformed beta is quite distinct in specimens quenched from high temperature. At lower temperatures it becomes increasingly difficult to distinguish the fine alpha plates. Illustrations of this point are found in Fig. 11 and 12, showing a clearly acicular structure in the beta areas at 980 ^{o}C and in Fig. 13 from 970 ^{o}C and Fig. 14 a from 900 ^{o}C where there is only an oriented roughness of the etched surface, and finally Figs. 14 b and 15 showing only an even roughness of the beta at 900 and 850 ^{o}C respectively. At 700 ^{o}C, Fig. 16, the residual beta has a bright even surface. These pictures were taken with ordinary light microscope, which could be suspected of being unable to resolve the details of the structure in question. However, electron microscope did not reveal anything more, as can be seen in Figs. 19 a - b from 900 and 875 ^{o}C respectively.

Precipitation of Secondary Phase.

In the beta plus alpha structure X first appears at the beta-alpha phase boundary as approximately equiaxed particles. Figs. 20 and 21 shows early stages of X formation in beta plus alpha at high temperature. The size of the particles is of the smallest order that can be resolved in the light microscope.

When the particles are located in the beta-alpha phase boundary no preferred direction of growth relative to the phase boundary can be detected. When observed in the ordinary light microscope, particles located at the phase boundary usually appear to grow to the same extent in both phases. When such a particle extends more into the alpha grain than in beta, the particles still have a spherical shape. The electron microscope reveals that the X particles, extracted together with the replica, have a branched structure, "dendrites".

Anyway it does not seem to be a preferred growth in any of the bordering matrix grains. When X is surrounded by alpha, this is rather an indication of an increase in amount of alpha simultanously with the growth of X. However, in the initial stage of cooperative reaction between beta, alpha and X the reaction takes the opposite direction. The lineal analysis has shown that while the alpha to beta ratio rises in the direction of lower temperature in the alpha plus beta region, the amount of alpha is again definitely less in the alpha plus beta plus X field immediately below it upper limit. In other words, at the initial precipitation of X during cooling from the beta plus alpha structure, the amount of alpha decreases.

To study this further the following experiment was made. Three β phase specimens were isothermally transformed to alpha plus beta at 900 ^{o}C for 20 min. The specimens were then allowed to cool in the annealing bath. When after 10 min. the temperature had reached 870 ^{o}C, one specimen was quenched. After another 6 min. the temperature was 850 ^{o}C and the second specimen was quenched. After a further 6 min. at 800 ^{o}C the third specimen was quenched. The first two specimens from 870 and 850 ^{o}C contained only alpha plus beta, but in the last one X particles also appeared. The interesting thing is that a great number of these particles were wholly surrounded by beta, but outlined the shape of the nearby beta-alpha phase boundaries in the wellknown manner. This phenomenon is shown in Fig. 22. Appararently these particles have been developed at the former phase boundary and then the alpha has shrunk leaving the X particles behind.

The same situation during isothermal transformation has been observed in the microscope. Fig. 23 shows a stage where a great number of the X particles are surrounded by beta phase. It is believed that the X particles have first formed at the beta-alpha phase boundary. This boundary has then retreated because the alpha phase has been consumed during the precipitation of X. In a later stage the three phase reactions can be expected to yield a final increase of alpha.

Longer times at constant temperature leads to an increase in diameter of the X particles. In Fig. 24 the structure at complete transformation is shown at high magnification. The X particles have a large variation in size, the largest ones being those formed in the last transformed areas. This is apparent from Fig. 25 where the last traces of beta (white areas) are partly surrounded by large X-particles. Some particles are elongated and seem to consist of two or more approximately spherical bodies which have joined, "agglomeration". When the particles expose a sufficiently large surface area their colour is found to be white. (The same was the colour of the secondary phase in the 0.75 % Zr-Sn alloy studied in the as cast condition, and in the alloys of modified zircaloy-2 composition, isothermally transformed at 750^{o} to obtain large particles. The colour is the same both when the etching removes part of the particles and when they are brought up in positive relief. On the other hand the secondary phase in zircaloy-2 before heat treatment is reddish. It proved possible to change the colour of the zircaloy-2 particles into white by a slight polishing which apparently removed a red surface layer. The particles observed in isothermally transformed specimens of zircaloy-2 may then be either of another kind or of another composition as in untreated zircaloy-2.) - The observations made in the present investigation do not allow any statement as to the nature of the particles called X.

As a summary of the description of X phase precipitation from beta plus alpha the following might be stated. X is nucleated at the beta-alpha phase boundary (possibly also at alpha grain (plate) boundaries). The particles of X grow from the phase boundary in all directions indiscriminately in both phases. At least in some places the reaction

involving beta, alpha and precipitating X is connected at an early stage with a decrease in amount of alpha but changes later, giving the overall process eutectoid character with increasing amounts of both alpha and X. In the first, transient stage alpha decreases and the beta-alpha phase boundary retreats leaving the X particles in a matrix of beta phase. When the alpha then grows the beta-alpha phase boundary may advance past the X-particles. The fact that in most structures the beta-alpha phase boundary is decorated by X particles is probably because the change in amount of alpha involved in the three phase reaction is small enough not to move the phase boundary to a visible extent. The quantative estimation of the progress of the reactions shown in Fig. 5 supports this rationalization of the observations in the microscope.

Turning to the precipitation of X from supersaturated alpha phase at low temperatures, this process is less completely followed in this investigation than the transformations at higher temperatures. Only a few isothermal annealings have been made to ascertain that X phase eventually precipitates from the alpha phase denoted as supersaturated. The particles of X appear mostly in the boundaries between the alpha plates but can also be found within an alpha plate, see Fig. 26.

A Special, Minor Precipitate.

At this point the occurence of a minor amount of relatively large, brilliantly white and hard particles will be mentioned. The particles were encountered occasionally with no obvious systematic relation to the heat treatment, apart from their absence in samples quenched from above the beta plus alpha range. The particles showed a high relief over the etched matrix. The relief was more pronounced when the proportions between HF, HNO_3 and glycerine in the etching solution was 20:20:60 than 10:60:60. Microhardness measurements showed that their hardness was appreciably higher than that of the matrix. The average Vickers value at 1 g load was 151 for the particles as compared with 116 for the matrix. Such particles often served as starting points for the formation of alpha plates, usually radiating from the inclusion, as illustrated in Fig. 21.

Judging from the irregularity in their occurence, their shape, size and colour, and their hardness and by excluding other possible alternatives, the particles are believed to be zirconium carbide. It is contemplated to carry out a study of this phase later with material which exhibits less variation in carbon content than the present alloy.

Alteration of the Widmanstätten Alpha Pattern.

Isothermal annealing at 700 and 800 °C exceeding that required for the complete transformation of beta altered the structure of the alpha matrix. Fig. 27 illustrates the phenomenon. At 700 °C 4 h the change had begun and at 8 h the new structure had spread over the major part of the specimen. The progress was in principle about the same at 800 °C although the rate was greater.

The change of the alpha matrix seems to start in the last transformed regions of the former beta grains. The first step seems to be a dissolution of some of the X particles, probably by coalescence. This makes the contact line between the alpha plates less distinct. Simultaneously the initially wrinkled outer envelope boundary of the colonies of alpha plates is levelled out. The plate structure is thus replaced by alpha grains of a more equiaxed shape which consume plate after plate by infiltration, making the plates both thinner and shorter, see Fig. 27. The central part of a plate is the first to change. The X particles, which earlier decorated the contact planes, between the former plates, are thus found in the last remnants of the former alpha.

The number of the resulting new grains is of the same order as the number of orientations of the Widmanstätten alpha plates. The largest new grains developed from the largest colonies of equidirected, equioriented alpha plates.

When the alteration of the alpha has advanced to a certain degree, one can observe a difference in the depth of etching between changed and unchanged areas of alpha. The front of the growing grains is usually smooth or sometimes rugged on a micron-scale.

As already mentioned some degree of coalescence among the X particles takes place. Where X particles have dissolved there is often a discoloration of the alpha, possibly caused by remaining concentrations of the alloying elements from X in alpha.

4. General Discussion.

Summary of Observations.

The products of isothermal transformation of the beta phase in zircaloy-2 have been found to be alloyed alpha zirconium and a secondary precipitated phase, called X. At different temperatures the transformation gives the following sequences of phases when passing from high to low temperatures: beta plus alpha between 980 and 880 ^{o}C, beta plus alpha plus X between 880 and 810 ^{o}C, alpha plus X between 810 and 500 ^{o}C and finally supersaturated single phase alpha below 500 ^{o}C. The transformation diagram shows an upper nose corresponding to the transformation to alpha and a lower nose reflecting the temperature dependence of X phase precipitation.

The alpha phase takes two forms. In the initial stages at high temperatures it occurs as a rim in the beta grain boundaries. The later formed major part of the alpha crystallizes as plates in Widmanstätten pattern. It has been found in the present investigation that the plates form by a shear mechanism, the size of the plates as well as the spacing between them decreases with decreasing holding temperature. In the completely transformed alpha structure coalescense takes place to a minor extent, leading to some increase in size of the plates. At longer annealing times there is a reformation of the alpha matrix resulting in the disappearance of the plate pattern.

The secondary X phase is precipitated from the beta plus alpha structure as small particles nucleated in the beta-alpha phase boundary. The beta-alpha-X reaction has an overall eutectoid character, but evidence has been obtained of a transient initial stage where the amount of alpha decreases during the precipitation of X. The size of the X particles is greater the later they form under the isothermal transformation. Longer heating times increases the average diameter. The size of the particles decreases with decreasing formation temperature.

The Widmanstätten Structure.

The use of the name Widmanstätten in describing the morphology of the alpha phase implies a similarity with other oriented, platelike precipitates which go under this name. It has therefore been considered proper to compare the Widmanstätten structure observed in zircaloy-2 with that in other systems.

First the occurrence of the Widmanstätten pattern in zircaloy-2 under practical conditions will be dealt with. The Widmanstätten plates are the alternative to equiaxed grains. The latter are the most common form in commercial material manufactured by deformation and subsequent annealing. The Widmanstätten figure on the other hand occurs whenever the alloy has been heated into the beta range and then cooled relatively fast. This happens in welding, a procedure which at present is regularly involved in the fabrication of fuel elements. It therefore seems to be inevitable that Widmanstätten alpha structures will be encountered sufficiently often to deserve attention with regard to their mode of formation and their mechanical properties.

Alternative and coexisting forms of crystallization, non-Widmanstätten and Widmanstätten, have been observed earlier in other systems, particularly hypoeutectoid steels. Ferrite forms from austenite either as a network in the grain boundaries of the matrix or as Widmanstätten plates inside the grains or both. The chronological order between these two forms is the same in low carbon steels as in zircaloy-2, first the grain boundary deposit and then the Widmanstätten plates. This is the rule in steels both during isothermal transformation (22, 23) and continous cooling (24, 25). (The grain size of austenite has been found to influence the mode of ferrite crystallization in the way that increasing grain size favours the Widmanstätten type. As to the cooling rate a high rate also gives more Widmanstätten plates). A difference in appearance of the two types of structures in steel and zircaloy-2 respectively may be noted, however. The rim of grain boundary ferrite has a less uniform thickness than the alpha rim in zircaloy-2, the ferrite grains having convex and sometimes angular sides towards the austenite. The Widmanstätten plates which grow from the grain boundary ferrite

are thicker at the base in relation to the length ("sawteeth") than the alpha plates in zircaloy-2. There is thus a difference between the grain boundary sideplates of ferrite and the elongated interior plates, which does not have any correspondance in zircaloy-2.

The observation of identical lattice orientation in the sideplates extending from a grain boundary rim into both the adjacent beta grains, disregarding the difference in lattice orientation of the latter, is in conflict with the common view that a Widmanstätten precipitate shall have a strict lattice relationship with the matrix. That the formation of plate alpha takes place by a shear mechanism is to be expected from the similar observations in other zirconium alloys, reported in the literature review, as well as in Widmanstätten structures in general. The same is true about the absence of indications of shear in the rim alpha. It is conceivable that a transformation controlled solely by diffusion could dominate at the higher temperature, where the rim is formed, and a shear process at a lower. The latter process, although it has greater growth rate, requires a larger nucleation energy. This can be obtained only at larger degree of undercooling. Another factor which possible may have some importance is the fact that at lower temperatures a process completely governed by diffusion is hampered both by a lower rate of migration of individual atoms and by the fact that greater number of atoms have to be transported by diffusion, since the difference in composition between the matrix and the precipitated phase most probably increases with decreasing temperature.

The fact that the formation of the Widmanstätten alpha plates takes place by a shear mechanism does not exclude diffusion as a step during the transformation. On the contrary it is rather likely that, in analogy with the formation of bainite by the same type of reaction, the shear is preceded by diffusion of some of the dissolved elements in order to facilitate the shear. It should then be noted that an alpha plate does not need to be developed at one occasion by a continously advancing shear front, but probably forms stepwise with intervening periods of diffusion.

It was not considered necessary to prove that the alpha plates are formed by a shear mechanism also at lower temperatures than the one observed, 900 ^{o}C, since there is no alternative mechanism which could be more favoured by decreasing temperature than the shear process.

By a shear process the new phase develops as lenses with a coherent interface towards the matrix. From geometric reasons the whole of a matrix grain cannot be completely filled by such lenses. There must be small spaces between the first formed lenses where the remaining matrix phase transforms into new grains with less degree of coherence and less favorable stress distribution. A possible consequence of this will be dealt with later.

The significance of Widmanstätten structure for the mechanical properties of zircaloy-2 does not seem to have been fully investigated. However, there are some observations made on other Widmanstätten structures which will be discussed here. It is usually considered that Widmanstätten figures are associated with low ductility. This experience comes mainly from steel. It should be observed that a fair comparison between different forms of ferrite is rendered difficult by the fact that Widmanstätten ferrite in steel is accompanied by a eutectoid, the character of which changes simultaneously with the factors which govern the form of the ferrite (25). Nevertheless the room temperature ductility of Widmanstätten alpha in zircaloy-2 can be expected to be inferior to that of equiaxed alpha. At high temperature on the other hand, there are indications that a Widmanstätten structure has a higher resistance to high temperature creep than equiaxed matrix grains. This is true, namely, both in steels (25) and in titanium alloys (27). Furthermore unalloyed zirconium annealed in the beta region has been found to show a significantly larger creep rupture stress than when annealed in the alpha region (28). The effect was ascribed to the more irregular grain boundaries in the former case, which most certainly were caused by crystallization of the alpha phase as Widmanstätten plates, forming groups with a scalloped envelope.

It is concluded from the discussion on this point that zircaloy-2 is similar to other alloys with respect to the formation of Widmanstätten figures and related types of structures. It is likely that the Widmanstätten alpha may have inferior ductility at room temperature than equiaxed grains, but probably has a higher creep rupture stress at high temperature.

The Alteration of the Widmanstätten Alpha Structure.

The disappearance of the Widmanstätten pattern during long time annealing at 700 and 800 ^{o}C is interesting both from practical and phenomenological viewpoint. In practice this process can be expected to occur when a zircaloy-2 ingot, which after having cooled from the molten state at a rate producing a relatively coarse Widmanstätten structure, is reheated for forging.

It has been observed earlier (2) that a fine Widmanstätten alpha pattern in zircaloy-2, obtained by quenching from beta, "recrystallizes" during subsequent annealing at 750 and 800 ^{o}C. After 2 h and 15 min. respectively the structure was almost completely replaced by large new grains. It was noted that the "recrystallization" eliminated so-called "stringers" i.e. rows of large particles of secondary precipitated phase. No other observations on the behaviour of the secondary precipitate were reported and the microphotos shown were taken on unetched surfaces with polarized light.

The fact that the alteration process starts in the last transformed regions of the beta grains is believed to be due to the lower degree of coherency and smaller strain energy in these regions.

It is not clear to what extent the X phase influences the changes of the matrix. It is plausible that the secondary phase(s) will change composition during annealing. The particles in general do most certainly not have the equilibrium composition characteristic for the temperature. Furthermore there is a segregation during the transformation causing the last formed particles to develop from a matrix of another composition than the older particles.

Composition changes may be partly responsible for the difference in etching behaviour between the old and the new matrix. A similar difference was observed in specimens which had accidently been transformed to Widmanstätten plates at two temperatures. The plates formed at high temperature, expected to have a higher Sn and a lower Fe (Cr, Ni) content than the others, etched deeper than the low temperature plates.

The Structure of Quenched Beta at High Degrees of Transformation

The lack of details in the observed structure of quenched beta at high degree of isothermal transformation could perhaps be attributed to the particular etching reagent used. Other etchants or polishing agents may possible cause a finer structure to show up in these regions. It remains true, however, that the ability of beta to transform into visible alpha plates decreases with decreasing quenching temperature. An extrapolation of this trend into a complete retention of beta to room temperature is not inconceivable. In the literature there are no data in support of this. The only relevant observation concerns the Zr-Fe system, where not even the very high iron contant of 5.5 weight procent could retain beta during quenching (29). - It is planned to study this problem further by X-ray analysis.

Precipitation of X Phase.

The analysis of literature data on the course of the three phase beta-alpha-theta reaction in the system Zr-Sn-Fe showed that theta should form from beta and alpha during cooling by a eutectoid transformation. The present investigation indicates that this is true also for the overall reaction of X formation in zircaloy-2.

The transient initial stage of X precipitation from beta plus alpha during which the amount of alpha decreases and that of beta increases is thought to be an adjustment to the equilibrium relation between the phases after the first precipitation of X from a supersaturated system has taken place. The X particles at the beta-alpha phase boundary appear quite late during the transformation and only a small amount of isothermal alpha is formed later. Also only few new particles are

precipitated after the first ones have grown to visible size. These facts explain why the X particles so clearly delineate the beta-alpha phase boundary at the moment of their nucleation.

The formation of X particles together with plates of alpha bears some resemblance to the bainite reaction in steel which takes place by shear type formation of ferrite accompanied by a precipitation of carbide in the ferrite. However, as pointed out above, the secondary phase in zircaloy-2 is found almost exclusively in the beta-alpha phase boundary.

As to the precipitation of X from supersaturated alpha phase, it should be observed that the incubation time found is most certainly affected by the existing stresses in the material. It is probable that with stresses greater than those caused by the cooling from 1050 ^{o}C, X will form quicker than by the rate shown in the transformation diagrams, Figs. 4 and 5.

Regarding the nature of the secondary precipitate called X it will again be emphasized that the observations in the microscope are admittedly incomplete, since they do not distinguish between possibly existing different kinds of secondary phases. It is tentatively suggested that some of the larger, white particles in the last transformed areas could be $ZrFe_2$ (or $ZrCr_2$ or Zr_2Ni) rather than theta. This is based on the conclusion from the phase diagram that the last transformed parts of the beta matrix during cooling has a considerably higher content of Fe and lower content of Sn than the matrix which precipitates the first X particles. It is hoped that the planned X-ray analysis and chemical analysis of extracted particles and X-ray microanalysis of the particles in situ will answer this question.

The Transformation Diagram.

The transformation diagrams in Figs. 4 and 5 exhibit some well known features and also some which call for special attention. There are two pronounced noses, one for the proeutectoid formation of alpha at high temperature and one for the precipitation of X. These noses are believed to have the same causes as usual in isothermal transformations

of this general type. The incubation time before the start of decomposition first diminishes with decreasing temperature due to increasing supersaturation. With lower temperatures, however, the mobility of the transforming elements decreases, giving rise to a minimum and below that an increase in the incubation time.

The shape of the curve for the start of alpha formation is reflected in the lines for various degrees of transformation in the beta plus alpha region. In the beta plus alpha plus X region the percentage curves conform to the shape of the curve denoting start of precipitation of X. This follows from the fact that, as already discussed above, the introduction of X in the beta plus alpha structure for a short while changes the course of the transformation process.

At lower temperatures the beta plus alpha region shrinks, i.e. the transformation into supersaturated alpha proceeds very fast, and at 500 ^{o}C and below no beta plus alpha structure was observed. The location of the border line between beta and supersaturated alpha is less precisely determined, as pointed out above. It seems however that a nose for supersaturated alpha in Figs. 4 and 5 at about the same temperature as for the X phase is likely.

The further extension of the same line downwards is still more obscure. It is an open question whether it shall mark a continous decrease in incubation time for supersaturated alpha below 300 ^{o}C, as indicated in this report, or, like in some steels, an increase followed above 200 ^{o}C by a discontinous interruption of a time-independent, completely diffusionless transformation.

It should be observed that the observations summarized in the transformation diagrams apply to zircaloy-2 of a particular, although fairly normal, composition. Other alloys might well give another picture and a more thorough investigation of the lower temperature ranges will probably provide the necessary background for a more definite idea of the transformation process.

5. Summary.

The high temperature beta phase in zircaloy-2 is transformed isothermally into the following sequence of phase combinations at equilibrium at different temperature:

$\beta + \alpha$ between 980 and 880 °C
$\beta + \alpha$ + secondary precipitate between 880 and 780 °C, and
α +, or supersaturated with, secondary precipitate below 780 °C.

The first alpha is formed as a rim in the beta grain boundaries. This is later superceded by Widmanstätten plates which are developed by a shear mechanism. The Widmanstätten alpha plates decrease in size and spacing with decreasing transformation temperature. They are grouped in colonies of equidirected members of the same lattice orientation. A colony has an approximately equiaxed extension and reacts as a single alpha grain with respect to twin formation. The Widmanstätten pattern of the alpha plates is altered by long time annealing into larger, more or less equiaxed alpha grains. (The Widmanstätten structure, which in practice is encountered in welds of zircaloy-2, is, from mechanical view point, probably characterized by a lower room temperature ductility as compared with equiaxed grains but a larger creep rupture stress at high temperature).

At high degrees of transformation the residual beta does not reveal any finer details in the quenched structure, with the etchant used.

The secondary precipitate is formed in the phase boundaries of the beta-alpha two phase matrix as small particles. The precipitation of the secondary phase occurs as a cooperative reaction together with the alpha phase. The overall character of the reaction is eutectoid. In an early transient stage the first precipitation of secondary phase causes a reversion of the balance between the amounts of beta and alpha so that the amount of alpha decreases.

The size of the particles of the secondary phase increases with isothermal holding time by agglomeration and coalescence, and decreases with lowered temperature. The secondary precipitate has not been identified with regard to composition and crystal structure.

At temperatures below 600 °C the beta is first transformed into a single phase structure of alpha which is supersaturated with the elements composing the secondary phase. The supersaturated alpha then rejects the latter phase.

The time-temperature-transformation diagram, which has been constructed on the basis of the observations in the microscope, has two noses for the curves indicating the beginning of the transformation of the beta phase: one for the proeutectoid alpha plus beta region and one for the alpha (plus beta) plus secondary phase region.

At the lowest temperatures studied the character and progress of the transformation of beta is less accurately known.

Acknowledgement

The interest and support of Dr R Kiessling, head of the Department of Materials Research and Development, Aktiebolaget Atomenergi, is gratefully acknowledged. Thanks are due to Sandvikens Jernverks Aktiebolag for the cold rolling of some material. The author is indebted to Messrs. A Brändström, E Broberg and B Lehtinen for their assistance in the experimental work and to Mr. G Lagerberg for valuable discussions.

6. Addendum.

Observations on Continously Cooled Specimens and a Comparison with Welds.

With the aim of correlating the above findings on isothermal transformations with the structures formed in welds of zircaloy-2 a few continous cooling experiments were made. Sheet specimens with 0.3, 0.8 or 7 mm thickness were beta-treated at 1050 °C in purified argon and then allowed to cool freely in various cooling media. To follow the temperature of the specimen a chromel-alumel thermocouple was attached to the specimen by riveting the hot junction into a small hole in the specimen. The thermocouple leads also served as a holder for the specimen when it was removed from the beta-treatment furnace.

The following cooling media were used: stationary air, air blast and boiling water. These media and the available sample dimensions allowed a variation of the mean cooling r te between 2200 and 23000 °C/min. in the range of interest, 1000 - 700 °C.

The structures obtained in the completely transformed specimens consisted of a matrix of Widmanstätten alpha plates, the size of which decreased with increasing cooling rate. A comparison with isothermally transformed specimens showed that most of the transformation during continous cooling had taken place between about 900 and 800 °C, i.e. in the lower part of the $\alpha + \beta + X$ region.

The continously cooled samples were also compared with the structure of welds. The welds observed were made between a 0.7 mm fuel element canning tube and its end plug. The welding was done in argon atmosphere with a tungsten electrode.

It was found that the structure in the molten and the heat affected zones was clearly acicular in contrast to the equiaxed grains of the virgin material. The former beta grains, developed during the welding, could be detected only occasionally by the existence of a grain boundary rim. The Widmanstätten alpha plates were grouped together in colonies as

described for isothermal transformation above, but this colony pattern was more pronounced in the welds. The colonies formed "grains," of approximately equiaxed shape. The size of the colonies decreased with increasing distance from the heat center of the welds.

The individual alpha plates were remarkably uniform in size throughout the whole weld, regardless of the size of the colonies. When compared with the continously cooled samples this alpha plate size in the welds was of the same order of magnitude as after cooling of 0.3 to 0.8 mm sheet in air blast.

It is realized from this study that continous cooling experiments of this kind gives only a rough idea of the transformation process in welds. The main difference lies in the thermal history before the cooling through the $\alpha + \beta$ region starts. This first part of the treatment determines the beta structure which in turn is responsible for the course of the transformation into alpha and secondary precipitate.

References.

1) RUBINSTEIN L S
Partial zircaloy-2-oxygen system
WAPD-ZH-15, May 1959, p. 5.

2) PICKLESIMER M L, ADAMSON G M
Development of a fabrication procedure for zircaloy-2
CF-56-11-115-1956. See WAPD-ZH-1, pp. 9-10 and ibid. -2, p. 23.

By the same authors also

Morphology of zircaloy-2
TID-7526 (Pt. 1), May 1956, pp. 165-185.

3a) INTRATER J
Dilatometric investigation of vacuum-melted zircaloy-2
WAPD-ZH-7, 1958.

b) MENDEL E, INTRATER J
Metallurgical studies of zircaloy-2
AECU-3976, 1959.

4) MEHAN R L, CUTLER G L
Thermal expansion of zircaloy-2 between room temperature and 1000 °C
KAPL-M-RML-15, 1958.

5) NOWIKOW A, PFEIFFER I
Schmelzen, Verarbeitung und mechanische Eigenschaften von Zircaloy-2
Ztschr. Metallkunde 48 (1957):8, pp. 479-482.

6) THOMAS D E, FORSCHER F
Properties of zircaloy-2
J. Metals 8 (1956):5, pp. 640-645.

7) NIEMANN J T, SOPHER R P
Embrittlement of multipass welds in zircaloy-2
Welding J 35 (1956):1, pp. 27-s-31-s. See also BMI-1006.

8) PERKINS F C
Metallographic investigation of commercial zircaloy alloys
AECU-3669, 1957. Abstract in N. S. A., 12 (1958):13, pp. 968-969, No. 8432.

9) MC GEARY R K
Dilatometric investigation of zirconium, zirconium-uranium, zirconium-oxygen and zirconium-nitrogen alloys
WAPD-36, 1951.

10) LANGERON J P, LEHR P
Préparation de gros cristaux de zirconium et détermination de l'orientation des precipités d'hydrure de zirconium
Rev. Mét. 55 (1958):10, pp. 901-906.

11) LANGERON J P, LEHR P
Sur l'étude de la transformation allotropique α⇌β du zirconium
Comptes rendus 247 (1958), Nov. 17, pp. 1734-1737. Abstract in N.S.A. 13 No. 3024
Also in Mem. Sci. Rev. Mét. 56 (1959):3, pp. 307-315.

12) CAIN F M
A simplified procedure for the metallurgy of zirconium and hafnium and their alloys
Zirconium and Zirconium Alloys, Amer. Soc. Metals. Cleveland, 1953. pp. 176-185.

13) GAUNT P, CHRISTIAN J W
The crystallography of the β - α - transformation in zirconium and in two titanium-molybdenum alloys
Acta Met. 7 (1959):8, pp. 534-543.

14a) TANNER L E
The system zirconium-iron-tin
ARF-2086-5, 1958. Abstract in N.S.A. 12 (1958):21, p. 1930. No. 15524.

b) TANNER L E, LEVINSON D W
The system zirconium-iron-tin
ARF-2068-4, 1958.

c) TANNER L E, SIMCOE C R
Studies of zirconium-iron-tin-alloys
ARF-2068-6, 1959.

d) TANNER L E, LEVINSON D W
The system zirconium-iron-tin
Amer. Soc. Metals, 1959. Preprint No. 166.

15) KUO K
Metallography of delta-ferrite
J. Iron Steel Inst. 181 (1955), pp. 223-325.

16) HILLERT M
Criterion for peritectic and eutectic reactions
J. Iron Steel Inst. 189 (1958), pp. 224-226.

17) TRECO R M, DICKERSON R F, ROTH H P
Report of metallographic committee on zirconium-base alloys
TID-5131, 1953, p. 12.

18) SCHRADER A
Ätzheft
Gebr. Borntraeger, 1957, p. 22. No. Fe 20.

19) MOLINDER G
Apparatus for linear microscopic analysis
Jernkont. Ann. 139 (1955):3, pp. 174-181. (Summary in English)

20) MODIN H, MODIN S
Pearlite and bainite structures in a eutectoid carbon steel. An electron microscopic investigation
Jernkont. Ann. 139 (1955), pp. 481-515.(in English.)

21) BERGSMAN B
Some recent observations in microhardness testing
Amer. Soc. Testing Materials Bulletin No. 176, 1951, Sept., pp. 37-43.

22a) MEHL R F
The decomposition of austenite by nucleation and growth process
J. Iron Steel Inst. 159 (1948:II), pp. 113-129.

b) MEHL R F, DUBÉ A
The eutectoid reaction
Phase Transformation in Solids, Symposium 1951.

23) PORTEVIN A, CONSTANT A, DELBART G
Conditions d´apparation de la structure de Widmanstätten dans le cas particulier d´un acier hypoeutectoide
Comptes Rendus 239 (1954), pp. 209-212.

24) HANEMANN H, SCHRADER A
Atlas Metallographicus
Berlin 1933, Gebr. Borntraeger.

25) ROSE A, KLEIN A
Der Ferrit in Widmannstättscher Anordnung
Stahl u. Eisen (1959):26, pp. 1901 - 1911.

26) MAZEL´ R YE
Effect of Widmanstätten pattern on the properties of low carbon boiler steel
Teploenergetika 2 (1958):1, pp. 37-40.
Abstract in The Abstracts Journal of Metallurgy 1958:10, p. 32, No. 79.

27) CROSSLEY F A, CAREW W F
Comparison of creep-rupture properties of Widmanstätten and equiaxed structures of Ti-7Al-3Mo alloy
Trans. Met. Soc. Amer. Inst. Met. Eng. 212 (1958):6, pp. 748-750.

28) GUARD R W, KEELER J H
Creep and stress rupture properties of zirconium. Effect of Annealing treatment
Trans. Amer. Soc. Metals 49 (1957), pp. 449-463.

29) HAYES E T, ROBERSON A H, O´BRIEN W
Constitution and mechanical properties of zirconium-iron alloys
Trans. Amer. Soc. Metals 43 (1951), pp. 888-904.

GÖ/EL

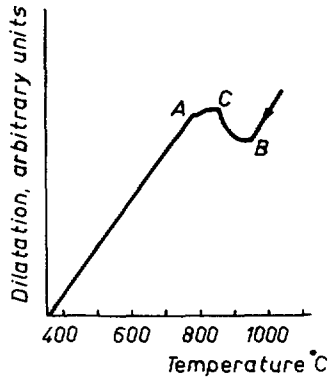

Fig. 1. Typical thermal expansion curve for zircaloy-2 according to Mendel & Intrater(3 b).
Conditions: Vacuum melted zircaloy-2, first heat treated at 1050°C 4 h and water quenched. Heating rate in dilatometer 100°C/h, cooling rate 100°C/h. B: beginning of transformation to α. C: start of precipitation of secondary phase. A: end of transformation to α.

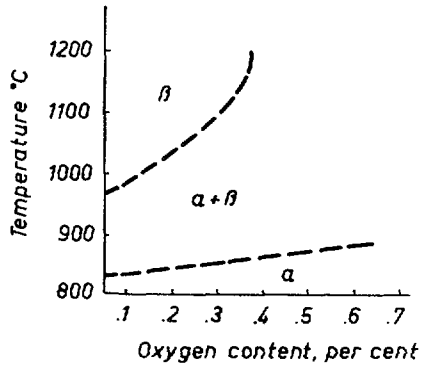

Fig. 2. Phase diagram zircaloy-2-oxygen according to Rubinstein (1).

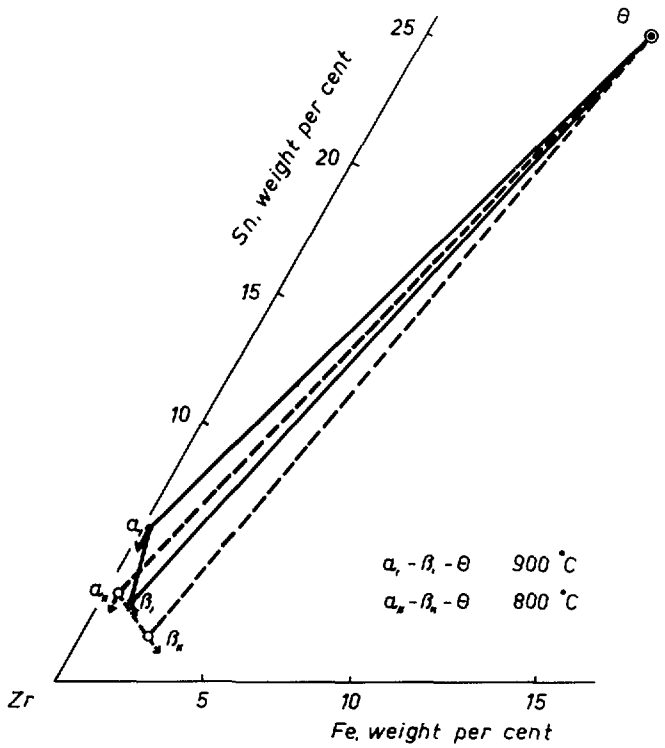

Fig. 3. The α-β - θ field in isothermal sections of phase diagram Zr-Sn-Fe at 900°C (full lines) and 800°C (broken lines) according to Tanner (15). Arrows at phase points indicate the change in composition on cooling.

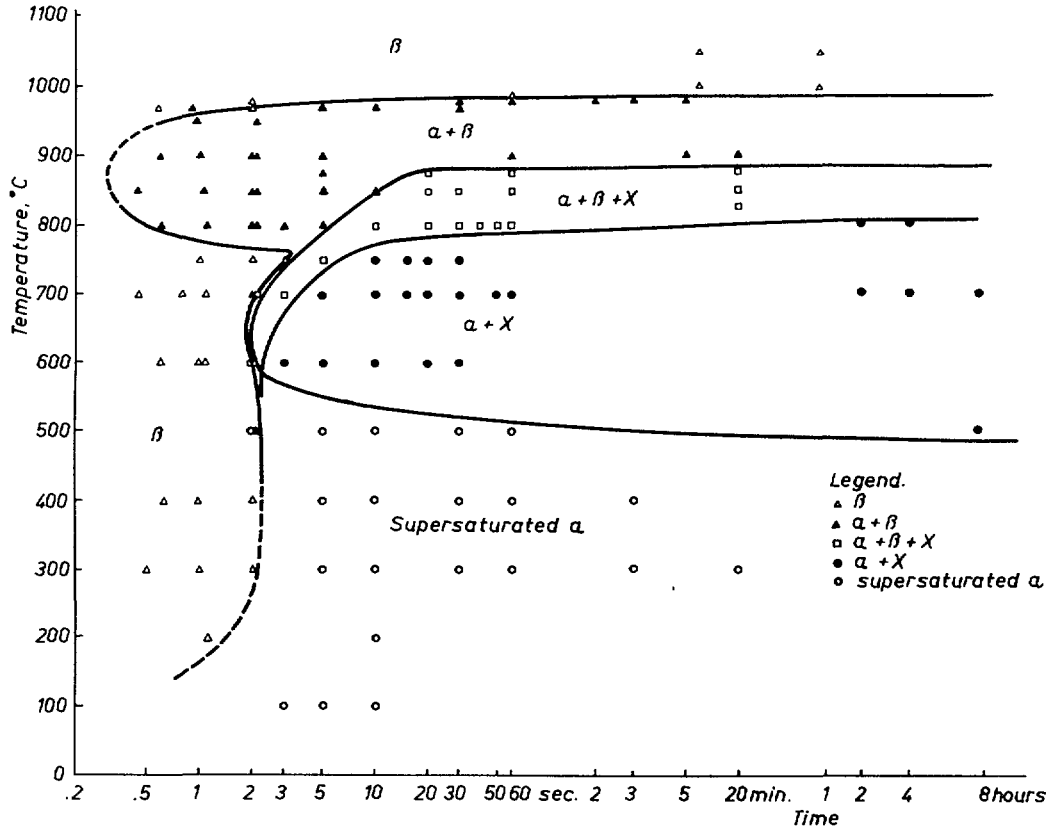

Fig. 4. Isothermal transformation diagram (TTT-diagram), microscopic phase determinations. All points refer to isothermal transformation after beta treatment at 1050°C, except at 1000 and 1050°C where the speciments were quenched directly from the high temperature.

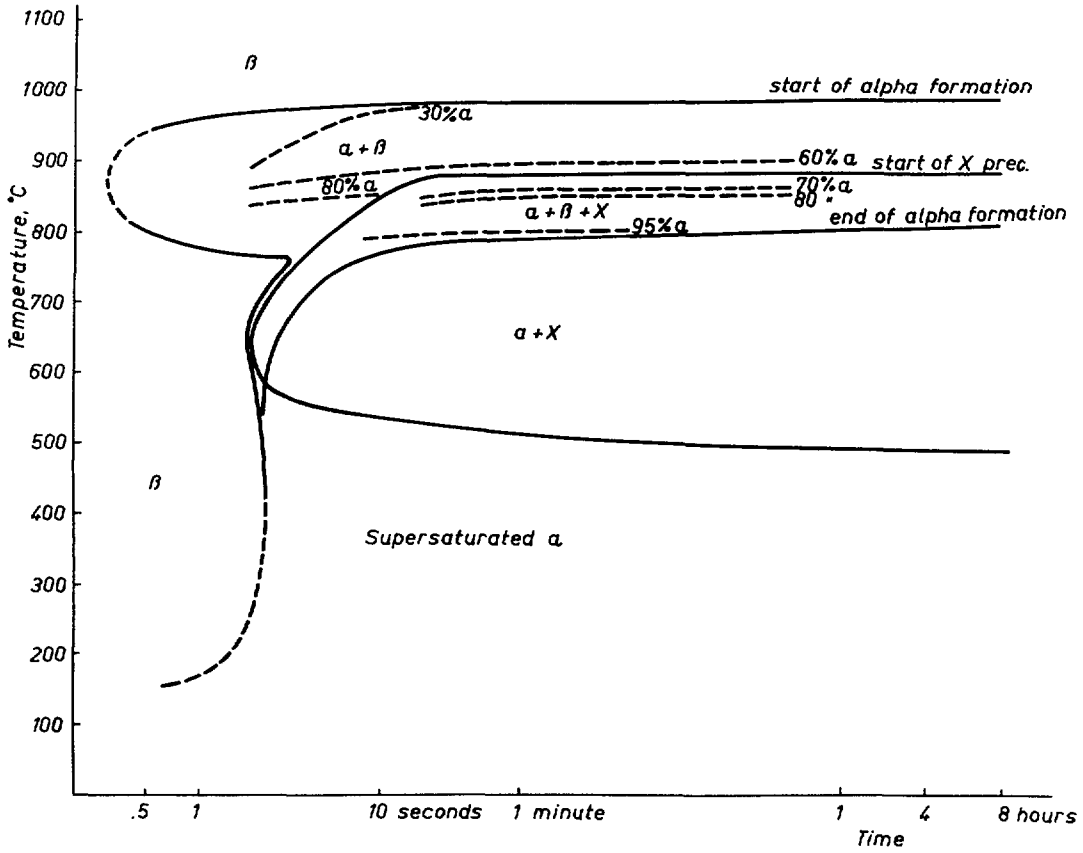

Fig. 5. Isothermal transformation diagram (TTT-diagram). Broken lines connect points with equal percentage of alpha in the matrix.

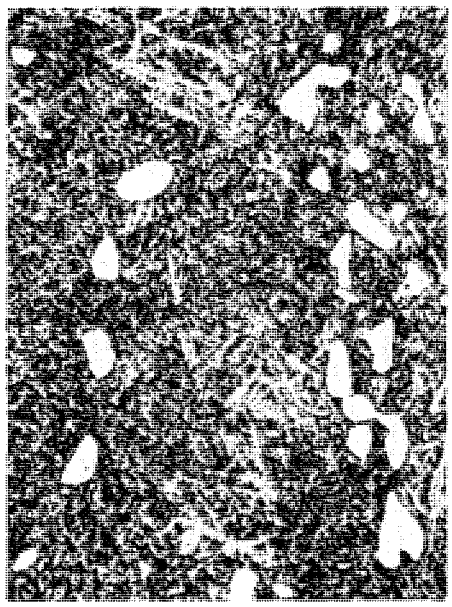

Fig. 6. 970° 12 min., w.q. ×600. Undissolved alpha (white) in matrix of transformed beta.

Fig. 7. 1050° 1 h., w.q. Unetched, polarized light ×150. Beta grains at 1050° transformed into areas of equioriented alpha plates.

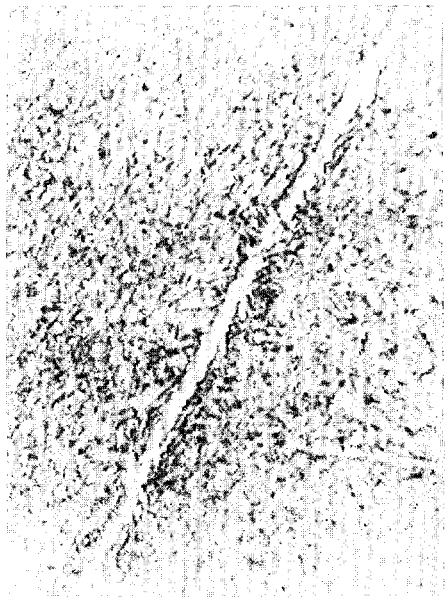

Fig. 8. 1050° 1 h., w.q. ×2000. Alpha as Widmanstätten plates and grain boundary rim.

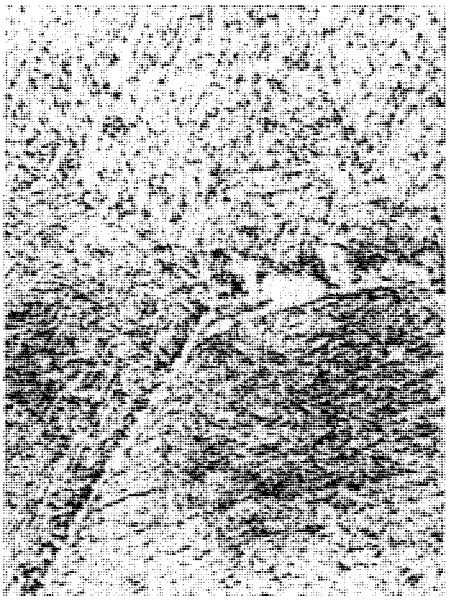

Fig. 9 a. 1050° 12 min., 980° 2 sec., w.q. ×2000. Alpha as Widmanstätten plates and grain boundary rim.

Fig. 9 b. 1050° 12 min., 980° 1 min., w.q. ×2000. Alpha as Widmanstätten plates and grain boundary rim.

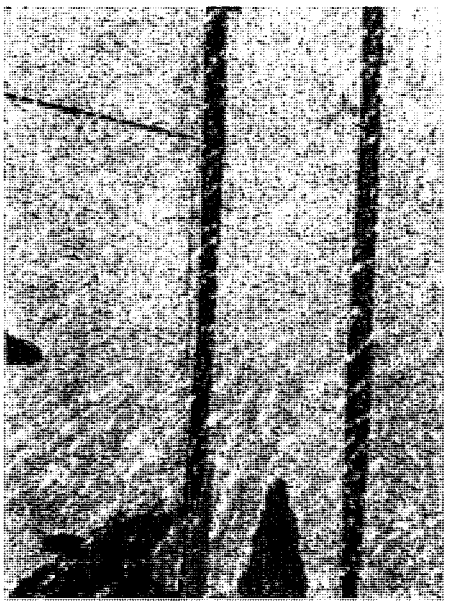

Fig. 10. Alloy of zirconium and 0.75 % tin as cast. Etched, polarized light ×500. Twins (dark bands) crossing a colony of alpha plates.

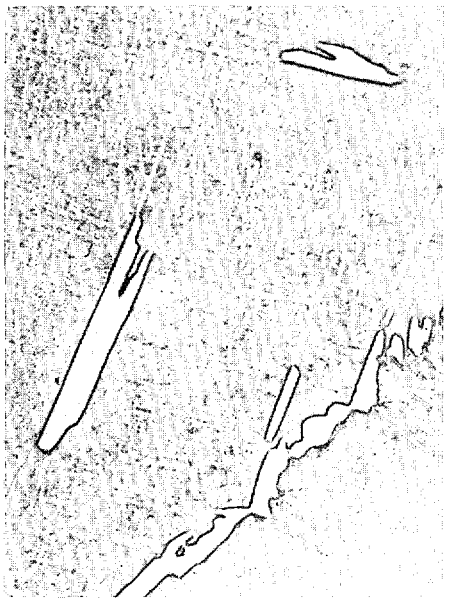

Fig. 11. 1050° 12 min., 980° 1 min., w.q. ×2000. Isothermally formed alpha plates and grain boundary rim with side plates.

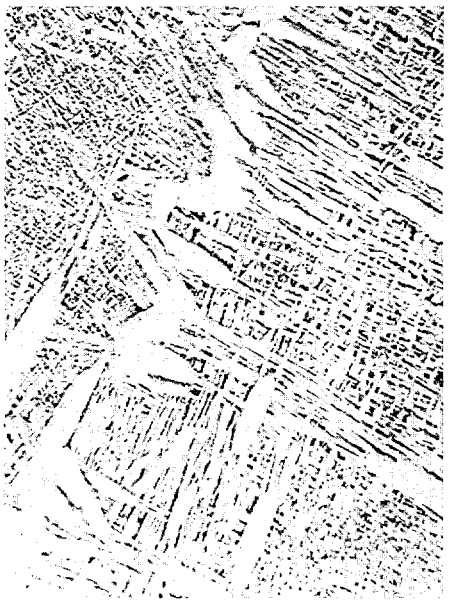

Fig. 12. 1050° 12 min., 980° 3 min., w.q. ×600. Widmanstätten alpha extending from grain boundary rim.

Fig. 13. 1050° 12 min., 970° 10 sec., w.q. ×600. Widmanstätten alpha plates and beta.

Fig. 14 a. 1050° 12 min., 900° 5 sec., w.q. ×600. Widmanstätten alpha plates and beta.

Fig. 14 b. 1050° 12 min., 900° 20 min., w.q. ×600. Widmanstätten alpha plates and beta.

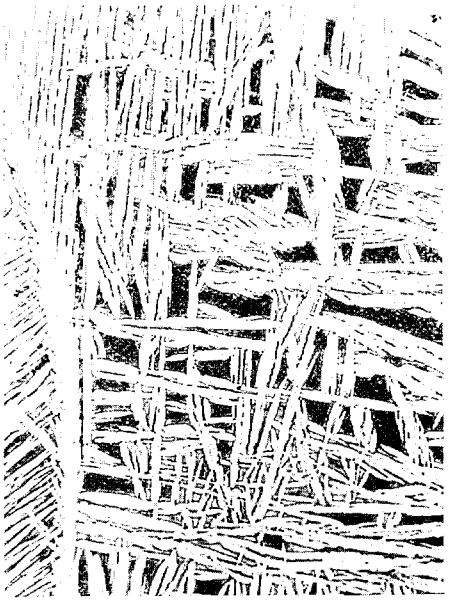

Fig. 15. 1050° 12 min., 850° 2 min., w.q. ×600. Widmanstätten alpha plates in a matrix of unresolvable structure.

Fig. 16. 1050° 12 min., 800° 5 sec., w.q. ×600. Isothermally formed coarse alpha plates and fine plates formed during the quench. The small squares between alpha plates were beta at 800°.

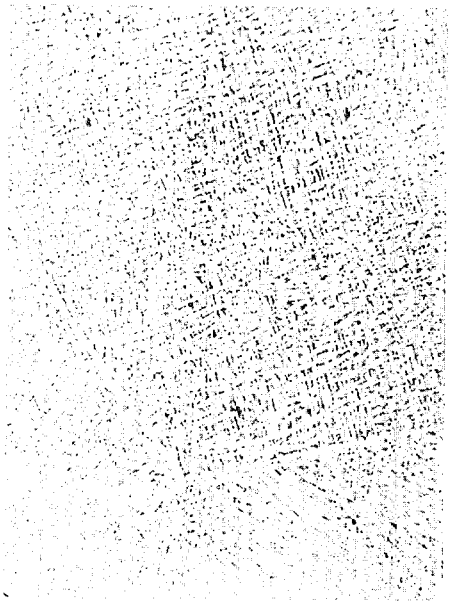

Fig. 17a. 1050° 12 min., 700° 2 sec., w.q. ×600. Isothermally formed, fine alpha and beta (at 700°).

Fig. 17b. 1050° 12 min., 700° 2 sec., w.q. ×2000. Isothermally formed, fine alpha and beta (at 700°).

Fig. 18. Heat treated in vacuum after polishing, 1020° 5 min., 900° 30 sec., cooled. Unetched ×2000. Alpha plates in relief on polished surface with originally straight fiducial lines.

Fig. 19 a. 1050° 12 min., a: 900° 20 min., w.q. electron microscope ×2800. Areas of beta at 900° (light grey) between plates of alpha (dark grey).

Fig. 19 b. 1050° 12 min., 875° 20 sec., w.q. electron microscope ×2800. Areas of beta at 875° (light grey) between plates of alpha (dark grey).

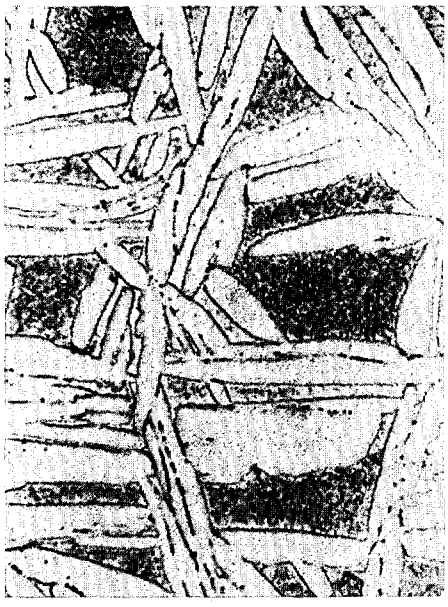

Fig. 20 a. 1050° 12 min., 875° 20 sec., w.q. normal light ×1200. Beta-alpha structure with beginning of precipitation of X as small particles at the beta-alpha phase boundary.

Fig. 20 b. 1050° 12 min., 875° 20 sec., w.q. electron microscope ×2800. Beta-alpha structure with beginning of precipitation of X as small particles at the beta-alpha phase boundary.

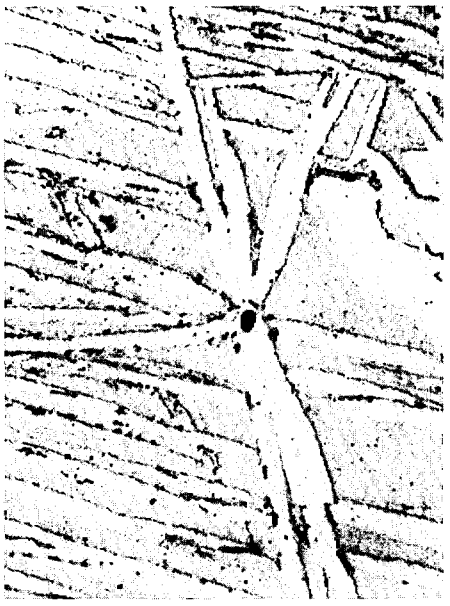

Fig. 21. 1050° 12 min., 875° 1 min., w.q. ×1200. Beta-alpha structure with beginning of precipitation of X as small particles at the beta-alpha phase boundary.

Fig. 22. 1050° 12 min., 900° 20 min., cooled slowly to 800° and w.q. ×2000. Rows of X particles in the beta areas delineating the former position of the beta-alpha phase boundary.

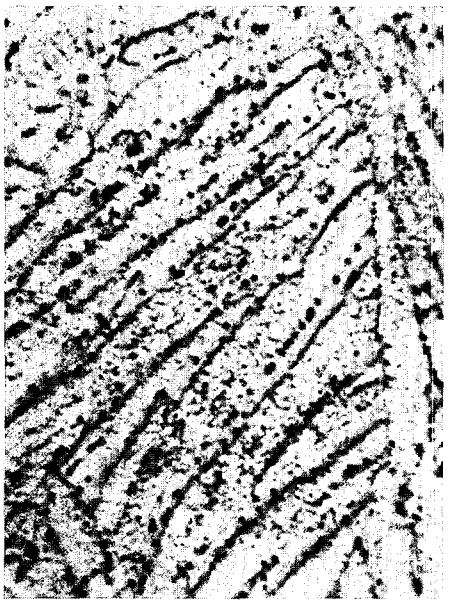

Fig. 23. 1050° 12 min., 800° 10 sec., w.q. ×2000. X particles near the beta-alpha phase boundary mostly surrounded by beta.

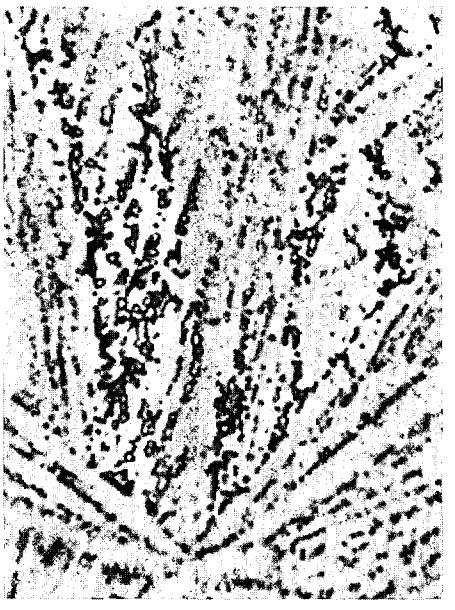

Fig 24. 1050° 12 min., 750° 30 sec., w.q. ×2000. Coarse particles of X phase of various sizes in the last transformed region.

Fig. 25. 1050° 12 min., 750° 5 sec., w.q. ×2000. Squares of beta (white) in last transformed regions with coarse particles of secondary phase.

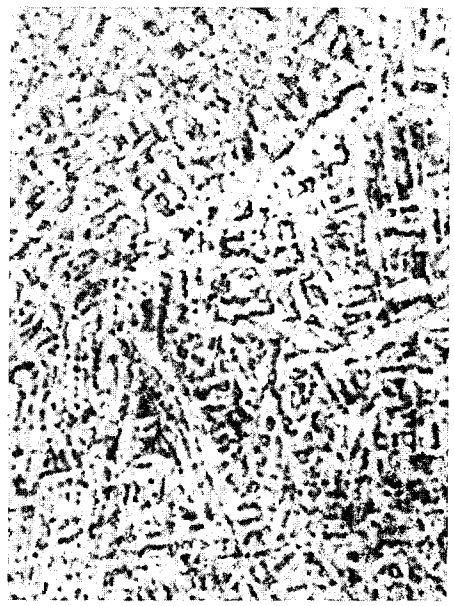

Fig. 26. 1050° 12 min., 500° 7 h 40 min., w.q. ×2000. X phase precipitated from supersaturated alpha.

Fig. 27. 1050° 12 min., 700° 8 h, w.q. ×2000. Alteration of Widmanstätten alpha (dark) into a new alpha matrix (white).

LIST OF AVAILABLE AE-REPORTS

Additional copies available at the library of
AB ATOMENERGI
Stockholm - Sweden

AE No	Title	Author	Printed in	Pages	Price in Sw. cr.
1	Calculation of the geometric buckling for reactors of various shapes.	*N. G. Sjöstrand*	1958	23	3
2	The variation of the reactivity with the number, diameter and length of the control rods in a heavy water natural uranium reactor.	*H. McCririck*	1958	24	3
3	Comparison of filter papers and an electrostatic precipitator for measurements on radioactive aerosols.	*R. Wiener*	1958	4	4
4	A slowing-down problem	*I. Carlvik, B. Pershagen*	1958	14	3
5	Absolute measurements with a 4π-counter. (2nd rev. ed.)	*Kerstin Martinsson*	1958	20	4
6	Monte Carlo calculations of neutron thermalization in a heterogeneous system.	*T. Hogberg*	1959	13	4
8	Metallurgical viewpoints on the brittleness of beryllium.	*G. Lagerberg*	1960	14	4
9	Swedish research on aluminium reactor technology.	*B. Forsén*	1960	13	4
10	Equipment for thermal neutron flux measurements in Reactor R2.	*E. Johansson, T. Nilsson, S. Claesson*	1960	9	6
11	Cross sections and neutron yields for U^{233}, U^{235} and Pu^{239} at 2200 m/sec.	*N. G. Sjöstrand J. S. Story*	1960	34	4
12	Geometric buckling measurements using the pulsed neutron source method.	*N. G. Sjostrand, J. Mednis, T. Nilsson*	1959	12	4
13	Absorption and flux density measurements in an iron plug in R1.	*R. Nilsson, J. Braun*	1958	24	4
14	GARLIC, a shielding program for GAmma Radiation from LIne- and Cylinder-sources.	*M. Roos*	1959	36	4
15	On the spherical harmonic expansion of the neutron angular distribution function.	*S. Depken*	1959	53	4
16	The Dancoff correction in various geometries.	*I. Carlvik, B. Pershagen*	1959	23	4
17	Radioactive nuclides formed by irradiation of the natural elements with thermal neutrons.	*K. Ekberg*	1959	29	4
18	The resonance integral of gold.	*K. Jirlow, E. Johansson*	1959	19	4
19	Sources of gamma radiation in a reactor core.	*M. Roos*	1959	21	4
20	Optimisation of gas-cooled reactors with the aid of mathematical computers.	*P. H. Margen*	1959	33	4
21	The fast fission effect in a cylindrical fuel element.	*I. Carlvik, B. Pershagen*	1959	25	4
22	The temperature coefficient of the resonance integral for uranium metal and oxide.	*P. Blomberg, E. Hellstrand, S. Hörner*	1960	25	4
23	Definition of the diffusion constant in one-group theory.	*N. G. Sjöstrand*	1960	8	4
25	A study of some temperature effects on the phonons in aluminium by use of cold neutrons.	*K-E. Larsson, U. Dahlborg, S. Holmryd*	1960	32	4
26	The effect of a diagonal control rod in a cylindrical reactor.	*T. Nilsson, N. G. Sjöstrand*	1960	4	4
28	RESEARCH ADMINISTRATION: A selected and annotated bibliography of recent literature..	*E. Rhenman, S. Svensson*	1960	49	6
29	Some general requirements for irradiation experiments.	*H. P. Myers, R Skjöldebrand*	1960	9	6
30	Metallographic Study of the Isothermal Transformation of Beta Phase in Zircaloy-2.	*G. Östberg*	1960	47	6
32	Structure investigations of some beryllium materials.	*I. Fäldt, G. Lagerberg*	1960	15	6
33	An Emergency Dosimeter for Neutrons.	*J. Braun, R. Nilsson*	1960	32	6

Affärstryck, Stockholm 1960